Hydrology and Earth System Sciences, 4(3), *483–498* (2000) © EGS

Hydrology & Earth System Sciences

Climatic and basin factors affecting the flood frequency curve: PART II—A full sensitivity analysis based on the continuous simulation approach combined with a factorial experimental design

M. Franchini[1], A.M. Hashemi[2] and P.E. O'Connell[2]

[1]Università degli Studi di Ferrara, Dipartimento di Ingegneria, Via Saragat 1, I-44100 Ferrara (I), Italy
[2]University of Newcastle upon Tyne, Department of Civil Engineering, Cassie Building, NE1 7RU, UK
e-mail for corresponding authors: mfranchini@ing.unife.it; ahmad.moaven-hashemi@ncl.ac.uk; P.E.O'Connell@ncl.ac.uk

Abstract

The sensitivity analysis described in Hashemi *et al.* (2000) is based on *one-at-a-time* perturbations to the model parameters. This type of analysis cannot highlight the presence of parameter interactions which might indeed affect the characteristics of the flood frequency curve (ffc) even more than the individual parameters. For this reason, the effects of the parameters of the rainfall, rainfall runoff models and of the potential evapotranspiration demand on the ffc are investigated here through an analysis of the results obtained from a factorial experimental design, where all the parameters are allowed to vary *simultaneously*.

This latter, more complex, analysis confirms the results obtained in Hashemi *et al.* (2000) thus making the conclusions drawn there of wider validity and not related strictly to the reference set selected. However, it is shown that two-factor interactions are present not only between different pairs of parameters of an individual model, but also between pairs of parameters of different models, such as rainfall and rainfall-runoff models, thus demonstrating the complex interaction between climate and basin characteristics affecting the ffc and in particular its curvature.

Furthermore, the wider range of climatic regime behaviour produced within the factorial experimental design shows that the probability distribution of soil moisture content at the storm arrival time is no longer sufficient to explain the link between the perturbations to the parameters and their effects on the ffc, as was suggested in Hashemi *et al.* (2000). Other factors have to be considered, such as the probability distribution of the soil moisture capacity, and the rainfall regime, expressed through the annual maximum rainfalls over different durations.

Keywords: Monte Carlo simulation; factorial experimental design; analysis of variance (ANOVA)

Introduction

Hashemi *et al.* (2000) showed through simulation experiments how, and to what extent, the flood frequency curve (ffc) is affected by the climatic (rainfall and evapotranspiration) regime and basin characteristics. While these findings apply to both unstandardised and standardised (by the mean annual flood) ffcs, the hydraulic and morphologic channel network characteristics affect only the unstandardised ffc. Furthermore, the results obtained suggest that the overall behaviour of the ffc is controlled by the probability distribution of the soil moisture at the storm arrival time (*SAT*).

The sensitivity analysis approach described in Hashemi *et al.* (2000) is based on '*one-at-a-time*' perturbations to the model parameters and, in what follows, will be referred to as *Simplified Sensitivity Analysis* (*SSA*). *SSA* cannot highlight the presence of parameter interactions which might, in turn, affect the characteristics of the ffc. Furthermore, when these parameter interactions are present, the effect of each parameter might be masked or altered by the levels assigned to the other parameters of the reference set.

Different approaches to sensitivity analysis have been described in the literature. Amongst the possible options considered for this study were Generalized Likelihood Uncertainty Estimation (GLUE) (Beven and Binley, 1992) which has been widely used for uncertainty analysis; hydrological applications are described in Freer *et al.* (1996) and Zak *et al.* (1997). However, GLUE focuses on parameter sets rather than on the behaviour of individual parameters and their interactions (Beven, 1998) and both GLUE and the technique described by Spear *et al.* (1994) have uncertainty analysis of model predictions as their main focus. Here, a sensitivity analysis of individual parameters and their interactions is the primary requirement, and predictive uncertainty is not considered. For this reason, a classical 'design of experiments approach' was adopted in which the 'experiment' is a set of Monte Carlo simulations

conducted with a set of model parameter combinations determined by a factorial design, where all the parameters are allowed to vary *simultaneously*.

The Analysis of Variance (ANOVA) technique is then used to analyse the results of the experiment, expressed in terms of variations in the ffc associated with the different parameter combinations. This more general and formal type of sensitivity analysis will be referred to be as *Full Sensitivity Analysis* (*FSA*), the objective of which is to determine whether the results observed in Hashemi *et al.* (2000) are general and not a function of the reference set of parameter values used in the *SSA*.

In implementing the *FSA* approach, the routing parameters, i.e. the celerity C, the diffusivity D and the width function shape and base length, will not be considered, since they do not affect the standardised ffc which is the main focus of the *FSA*. This reduces the number of parameters/factors to 13 and makes the computational load associated with the factorial experimental design more manageable.

The factorial experimental design approach to *FSA*

The term *experiment* is quite general and it indicates a test or a series of tests. The *design* of an experiment has a crucial role in the solution of the problem that initially motivated it. The *factorial experimental design* is a powerful technique (Montgomery and Runger, 1997) in which experimental runs are usually performed, in each complete trial or replicate, for all possible treatments or combinations of the levels of the factors (identified *a priori* as those affecting the 'system') and the response of the 'system' for each of them is measured/calculated. The term *factor* means an experimental variable, which influences a *response* or outcome of that experiment, and the term *level* refers to the value of the factor. The analysis of variance (ANOVA) technique is one of the primary tools used for the statistical analysis of the response of one or more replicates of an experiment. Moreover, graphical methods are used for the interpretation of the results of the experiment.

In general, all the factors can have several (more than two) levels. However, one of the most important cases of the factorial experimental design technique is that of k factors with each at only *two levels*. A complete replicate of such a design requires $2 \times 2 \times 2 \ldots . \times 2 = 2^k$ observations and is called 2^k *factorial experiment*. It provides the smallest number of runs for which k factors can be studied in a complete factorial design. However, because there are only two levels for each factor, it is assumed that the response is approximately linear over the range of the factor levels chosen.

The information given above is sufficient to create the basic link between the general theory of the factorial experimental design and the case under study. It is evident that, in our case, the 'response' of the 'system' has to be understood as *one* characteristic of the ffc. Of course, if more than one characteristic is needed to describe the properties of the standardised ffc, the ANOVA has to be repeated for each of them. The term 'factor' usually used in the context of the experimental design approach is equated here with the term 'parameter' as used in relation to the rainfall model, the potential evapotranspiration demand and the rainfall runoff model.

The results described in Hashemi *et al.* (2000) show, that, in all cases, a systematic variation of the characteristics of the standardised ffc is observed when these parameters are allowed to vary from the lower to the upper bound values, passing through their central/reference values. This situation justifies the use of the 2^k factorial experiment technique. However, as previously mentioned, this technique implies the assumption that the response is approximately linear over the range of the factor levels chosen. This may not be completely true in the case under study, but the experimental design approach provides the tools to give protection against curvature (Montgomery and Runger, 1997). At this point, there are two aspects to be discussed before presenting the results of the 2^k factorial experiment: (a) which structure of the 2^k factorial experiment has been selected for the current study and (b) which statistics have been used to describe the properties of the standardised ffc, i.e. the 'system response'.

(a) Selection of the structure of the 2^k factorial experiment

Before designing the experiment, a brief review of the fundamentals of the experimental design approach is necessary. As previously mentioned, in each complete trial or replicate of a factorial experiment, all possible combinations of the levels of the factors are considered and the corresponding 'response' of the 'system' measured. The *main effect* of a factor is defined as the *change* in response produced by a change in the level of the factor. Thus, for a generic factor A, its main effect is the difference between the average response at the high level of A (represented by $+1$ in Fig. 1) and the average response at the low level of A (represented by -1). Figure 1 shows graphically the meaning of the main effect of a generic factor. However, in some experiments, the difference in response between the levels of one factor is not the same at all levels of the other factors, i.e. the effect of the factor depends on the levels of the other factors. When this happens, there is an *interaction* between the factors. When the interaction is *large*, the main effects of the factors involved in the interaction *may* not have much meaning. The concept of interaction between two generic factors A and B can be illustrated through plots like Fig. 2. Figure 2a shows the response of the 'system' against the levels of A (denoted by $+1$ and -1) for both the high and low levels of B, which, for illustrative purposes, are designated in Fig. 2 as $B+$ and $B-$, respectively. In this

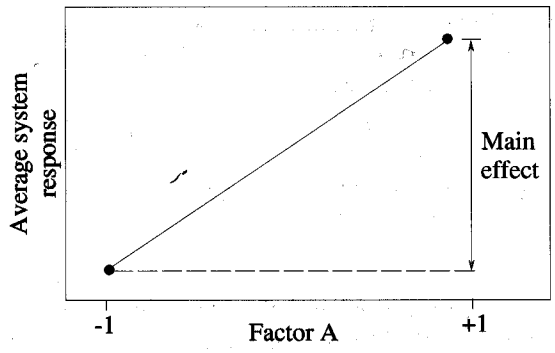

Fig. 1. *Representation of the meaning of the main effect of an individual factor (−1 and +1 stand for low and high levels of the factor respectively).*

case the $B-$and $B+$ lines are parallel, thus indicating that no interaction exists between the two factors. In fact, the main effect of A remains unchanged when the factor B changes from its low level to its high level. However, note that, in the case described, the 'response' of the system (not the main effect) is higher when the factor B is at its high level $B+$. Figure 2b shows a similar plot, but, in this case, the $B-$and $B+$ lines are not parallel, indicating the interaction between the factors A and B. In this case, the main effect of A now depends on the level of the factor B and vice versa.

To explain further the relevant terminologies, consider the above two factors, A and B, at high and low levels. Then there will be only $N = 2^2$ combinations of the factors (or *treatments*) contributing to the experiment. The four possible treatments to be examined, and the corresponding levels of the factors A and B, are shown in the design matrix in Table 1. Also shown in Table 1 is AB, the interaction between A and B, the sign of which is obtained by using the simple mathematical rule that plus (+1) times minus (−1) gives minus (−1) and minus (−1) times minus (−1) gives (+1).

The effect of each individual factor (main effect) and the two-order interaction effects on the system response can be determined through the use of the signs shown in Table 1

Table 1. The design matrix for a 2^2 factorial experiment.

Treatment	A	B	AB
1	−1	−1	+1
2	+1	−1	−1
3	−1	+1	−1
4	+1	+1	+1

Note: +1 and −1 represent the high and low levels of the factors, respectively.

according to the formula:

$$Effect_j = \frac{\sum_{i=1}^{N}(S_{ij} \times V_i)}{N/2} \quad (1)$$

where N is the total number of experimental runs or treatments, S_{ij} represents the sign in row i and column j and V_i represents the response value obtained from the corresponding treatment/factor combination. According to this rule and considering the design matrix in Table 1, the effect of each factor and two-order interaction can be calculated as follows:

$$Effect_1(\textit{main effect of factor } A) = 1/2[-V_1 + V_2 - V_3 + V_4];$$

$$Effect_2(\textit{main effect of factor } B) = 1/2[-V_1 - V_2 + V_3 + V_4];$$

$$Effect_3(\textit{two-order interaction } AB) = 1/2[+V_1 - V_2 - V_3 + V_4]$$

As the number of factors in the factorial experiment grows, the number of effects that can be estimated also grows. In the current case, a 2^{13} experiment should be performed with $n \geq 2$ replications. Table 2 shows the number of main effects and the number of two and higher order interactions.

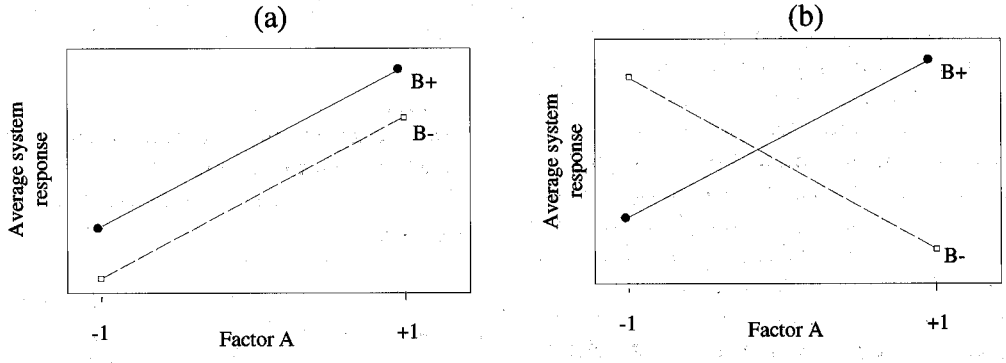

Fig. 2. *Representation of the system response to variations of factors A and B: (a) absence of two-factor interaction effects; (b) presence of two-factor interaction effects.*

Table 2. Number of main effects and high order interactions for the 2^{13} factorial design.

	Main effect	Interaction order											
		2	3	4	5	6	7	8	9	10	11	12	13
Number of effects	13	78	286	715	1287	1716	1716	1287	715	286	78	13	1

It can be realised that, although such a full experiment would be able to provide the information about all the interaction effects, it is computationally intensive, and most of the high order interactions are, in practice, impossible to iterpret. Moreover, in such a situation, *the sparsity of effect principle* applies: that is, the system is expected to be dominated by the main effects and low-order interactions, and thus, the higher order interactions are expected to be negligible (Montgomery, 1997; Box *et al.*, 1978).

Therefore, when the number of factors is large, a common practice is to run only a *single replicate of the* 2^k *factorial experiment* and then pool the higher order interactions as an estimate of error, i.e. the higher order interactions are considered as noise in the linear regression (Montgomery and Runger, Chapter 13, 1997) and thus their *SS* (Sum of Squares) is treated as a normally distributed error with zero mean and variance σ^2.

However, even if a single replicate of the experiment is made, in the current case $2^{13} = 8192$ runs have to be performed. For the *SSA*, each run involves the generation of a 10000 year sequence of discharges at an hourly level and it is thus evident that such an approach cannot be applied.

A possible solution to this problem is given by the 2^k *fractional factorial design*. In fact, once accepted *a priori* that certain high order interactions are not of interest, then a *fractional factorial design* involving fewer than a complete set of 2^k runs can be used to obtain information on the main effects and low-order interactions. The reduction of the number of runs can be very important depending on the type of fractional factorial design selected. Basically, a 2^{k-p} fractional factorial design contains $1/2^p$ runs of the full 2^k factorial design, and therefore, a 2^{k-1} fractional factorial design contains a one-half fraction of the runs of a full 2^k factorial design.

Since, in a fractional factorial design, only a sub-set of all possible treatment combinations of the several factors are considered, it is fundamental to define *which combinations* have to be considered. The theoretical problem behind this choice is the 'confusion' in the identification of the effects of the single factors and interactions. In other words, it is said that such parameters are aliased with each other and, at the end of the fractional experiment, what is calculated may not be only the effect of a factor A, for example, but it may include the sum of the effects of the factor A and of some other interactions (depending on the design resolution).

To clarify the concept of aliases, consider a 2^3 full factorial experiment. From such an experiment, 3 main effects, 3 two-factor interactions and 1 three-factor interaction can be calculated. However, from a half-factorial design (2^{3-1}), some effects are indistinguishable from each other (Table 3). It may be realised from Table 3 that the column labelled A has an identical pattern with that of BC, B with AC, and C with AB (note that Table 3 represents a half set of the possible treatments that comprise a full 2^3 experimental design). As a consequence, the effects, for example, of A and BC, when calculated with Eqn. 1, cannot be distinguished, or rather, what is calculated is the sum of their effects. Therefore, since the effects cannot be separated from each other, the fractional factorial experiment must be designed carefully to achieve meaningful results. When aliases are present, it is usually considered that lower order effects are more important than those of higher orders. Moreover, depending on the resolution of the factorial design, the aliases might be between single factor and two-factor interactions, two-factor interactions and three-factor interactions or other two-factor interactions, and so on.

However, to minimize such problems and bearing in mind the sparsity of effect principle, it is important to build up the experiment in such a way that the main factors are *aliased* with high order interactions, the effect of which are expected to be negligible. In this way, the estimated effect is mainly due to the main factor and can be considered as a reliable estimate of it. In this context, the concept of *design resolution* is fundamental to classifying fractional factorial designs according to the alias pattern they produce. Designs of resolution *III*, *IV* and *V* are of particular interest. For example, a 2^{k-p} fractional factorial design with resolution *IV* (usually indicated with the symbol 2^{k-p}_{IV}) is that in which no main effect is aliased with any other main effect or two-factor interactions, but some two-factor interactions can be aliased with each other. This implies a preliminary

Table 3. Notation for calculating effects in the 2^{3-1} fractional factorial experiment.

Treatment	A	B	C	AB	AC	BC	ABC
a	+1	−1	−1	−1	−1	+1	+1
b	−1	+1	−1	−1	+1	−1	+1
c	−1	−1	+1	+1	−1	−1	+1
abc	+1	+1	+1	+1	+1	+1	+1

Table 4. The factorial design matrix.

Run	*A*	*B*	*C*	*D*	*E*	*F*	*G*	*H*	*J*	*K*	*L*	*M*	*N*
1	−1	−1	−1	−1	−1	−1	−1	+1	+1	−1	−1	+1	−1
2	+1	−1	−1	−1	−1	−1	−1	+1	+1	−1	+1	−1	+1
3	−1	+1	−1	−1	−1	−1	−1	+1	−1	+1	+1	+1	+1
.	.	.	.	.	.	.	.	.	.	.	.	.	.
.	.	.	.	.	.	.	.	.	.	.	.	.	.
.	.	.	.	.	.	.	.	.	.	.	.	.	.
128	+1	+1	+1	+1	+1	+1	+1	+1	+1	+1	+1	+1	+1

identification of the two-factor interactions which are expected to be the most and least important, in order to avoid that important two-factor interactions are aliased with other important two-factor interactions.

On the basis of the considerations presented above, a $1/2^p$ fraction of a 2^k factorial design with resolution *IV*, i.e. a 2^{k-p}_{IV} experiment, has been selected. In this context, the package MINITAB was used to set up this type of experiment, and a value of $p = 6$ was selected, giving a total of 128 runs. The value of $p = 6$ represents a compromise between resolution and computational effort. Table 4 shows some of the treatments designed for the proposed fractional factorial experiment. The numbers −1 and +1 indicate that the corresponding factor is considered at its low or high value, respectively, in the current run. Table 5 shows the list of the aliases up to the third order. Note that the main factors are aliased only with the third-factor interactions, while the two-factor interactions are mainly aliased with the third-factor interactions except in six cases. Considering that there are 78 two-factor interactions when $k = 13$ and that this structure may create some doubts on the interpretation of the two-factor interaction effects only in six cases, it can be concluded that the structure of this experiment is acceptable. However, to minimize the negative effects of these aliases among the two-factor interaction effects, an *a priori* selection of the parameters to be assigned to the different letters shown in Table 5 was performed on the basis both of the results of the *SSA* described in Hashemi *et*

Table 5. Alias Structure up to order 3. See also Table 6 for the meaning of the letters.

Main effect aliases with higher order interactions	Some 2-order interactions aliases with higher order interactions
A + BCN	DE + FGH + FJK
B + ACN	DF + EGH + EJK
C + ABN	DG + EFH
D	DH + EFG
E	DJ + EFK
F	DK + EFJ
G + HJK	DL + AMN + BCM
H + GJK	DM + ALN + BCL
J + GHK	DN + ALM
K + GHJ	EF + ACM + BMN + DGH + DJK
L	EG + AJN + BCJ + DFH
M	EH + AKN + BCK + DFG
N + ABC	EJ + AGN + BCG + DFK
	EK + AHN + BCH + DFJ
Alias structure of 2-order interactions with 2 and higher order interactions	EL
AB + CN + GHL + JKL	FK + DEJ + GLM
AC + BN + EFM	FL + GKM + HJM
AN + BC + DLM + EGJ + EHK	FM + ACE + BEN + GKL + HJL
GH + JK + ABL + CLN + DEF	FN + BEM
GJ + HK + AEN + BCE	
GK + HJ + FLM	

Table 6. Links between letters (see Table 5) and model parameters.

Designation	*A*	*B*	*C*	*D*	*E*	*F*	*G*	*H*	*J*	*K*	*L*	*M*	*N*
Parameter	ETp	β	η_1	λ	α	W_m	η_2	ξ_2	ν	d_2	b	d_1	ξ_1

al. (2000) and the physical meaning of the parameters, (see Table 6). From Tables 5 and 6, it is possible to observe the aliases for the two-factor interactions: for example, the two-factor interaction effect of $(\eta_2\xi_2)$ is aliased with that of (νd_2), or, in other words, the effect calculated for the interaction $(\eta_2\xi_2)$ is indeed the sum of the effects of the two-factor interactions $(\eta_2\xi_2)$, (νd_2) and higher order interactions. The design has been verified *a posteriori* through the analysis of the interactions really observed and it appears that the design is correct since no significant interactions were observed among the parameters selected for the aliases and thus no information was lost.

To obtain a better estimation of the experimental error, and perform a more reliable analysis of variance, the 2^{13-6}_{IV} experiment was replicated twice using a different seed for the generation of the time series of rainfall and evapotranspiration demand. In order to protect against the problem of curvature in the response, a central point in the parameter domain was also considered (Montgomery and Runger, 1997) but the low statistical significance of this latter point suggested that the hypothesis of approximately linear response over the range of the factor levels chosen is acceptable.

From each series, which was limited to a length of 1000 years for computational reasons, a set of statistics was extracted on which the ANOVA was performed. The third-order interaction effects were assumed to be negligible and their Sum of Squares (SS) was pooled with the Sum of Squares of Errors (SS_E) available from the two replications.

Once the factorial experiment has been performed and the main effects and interactions calculated (see, e.g. Montgomery and Runger, 1997) it is necessary to evaluate whether these main and interaction effects are statistically significant. The standard approach makes use of the *analysis of variance* technique which, in this case, is applied to the 'system response' i.e. the ffc.

(B) SELECTION OF THE STATISTICS TO BE USED IN THE ANOVA

To decide how to quantify the resulting change in the ffc due to the perturbation to the several parameters, it is important to observe that, for example, an upward shift of the standardised ffc may be a consequence of a combined scale/shape effect. In fact, as mentioned in Hashemi *et al.* (2000), any three-parameter distribution, such as the GEV, Pareto or Generalized Logistic, can be described by a location parameter, a scale parameter and a shape parameter (Hosking and Wallis, 1997). When the ffc is standardised by the mean annual flood, the quantiles will be a function of both the scale and shape parameters, and determined by *L-CV* and *L-CS* statistics. However, the shape parameter tends to be uniquely related to *L-CS* and gives a measure of the curvature of the ffc.

Due to this fact, the *FSA* cannot be applied separately, at least *a priori*, either to *L-CV* and *L-CS* statistics or to the scale and shape parameters of a selected probability distribution, because the results, in terms of upward/downward shift, might not be univocal. For this reason, the set of statistics to be used for the *FSA* was identified as a selected group of standardised quantiles (namely x_{10}, x_{50}, x_{100}, x_{500}, x_{1000}, where $x_T = Q_T/m_Q$) estimated from a GEV distribution fitted to the series of annual maximum values for each treatment. These quantiles can describe, in discretised form, the whole standardised ffc, thus giving information on possible upward/downward shifts and variations of the curvature.

The GEV distribution was selected through the analysis of the *L*-moment ratio diagram proposed by Hosking and Wallis (1997), shown in Fig. 3, where the *L*-kurtosis is plotted against the corresponding *L-CS* value. In this diagram any three-parameter distribution with location, scale and shape parameters can be represented by a curve defined by different values of the shape parameter. The

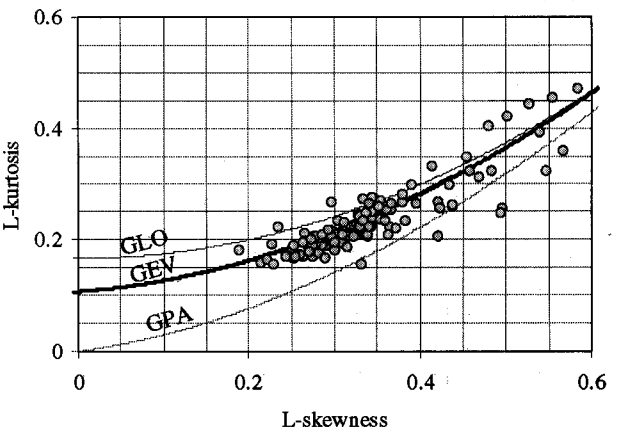

Fig. 3. *L-moment ratio diagram obtained from the series generated in the full sensitivity analysis (FSA).*

curves relevant to the GEV (Generalised Extreme Value), GLO (Generalised Logistic) and GPA (Generalised Pareto) distributions are represented in the plot together with the estimated pairs of third and fourth order *L*-moments corresponding to the many parameter combinations defined by the fractional factorial experiment. The overall distribution of these sampling points suggests that the GEV distribution is the most appropriate descriptor of the synthetic data.

In addition to the quantiles, the $L\text{-}CS_Q$ statistic (the value of which directly quantifies the curvature) and the mean m_Q of the annual maximum floods (the value of which quantifies the position of the ffc) were also calculated and the ANOVA was applied to all these statistics and the main effects, two-factor interaction effects and the P-values measuring their significance were calculated (Montgomery, 1997).

The analysis of all these results has shown that for the standardised ffc, a systematic coherence is observed between the results (main and two-factor interaction effects) for the quantiles of different return period, x_T, and those observed for the curvature described by the $L\text{-}CS_Q$ statistic (recall that the quantiles describe in discretised form the standardised ffc and thus its curvature). For this reason, the subsequent discussion will be presented with reference to this latter parameter combined with the analysis of the results for the statistic m_Q, which represents the link between the unstandardised and standardised ffcs. Therefore, in what follows, attention will be focused on the properties of the ffc characterising its position/location (m_Q) and its curvature ($L - CS_Q$). Furthermore, for an easier and more readable presentation, only the graphical output of the ANOVA will be shown.

Discussion of the results of the fractional factorial experiment

STATISTIC M_Q:MAIN EFFECTS AND TWO-FACTOR INTERACTIONS

Figure 4a shows the values of the mean m_Q observed in the *SSA*, where each parameter is perturbed *one-at-a-time*. Figure 4b shows the corresponding main effects of the different parameters observed in the *FSA*. On the x-axis, the values -1 and $+1$ represent the lower and the upper limit of each parameter, while on the y-axis the m_Q values are represented. The analysis of Fig. 4 suggests three considerations:

(a) the general level of m_Q observed in the *FSA* is higher than that observed in the *SSA*;
(b) the type of (main) effect of each parameter on the mean m_Q is the same both in the *SSA* and the *FSA*; in fact the slope of the segments linking the values of m_Q for the upper and lower limits of the several model parameters is always the same;
(c) the range of variation of the statistic m_Q in the *FSA* is very similar to that observed in the *SSA*.

As regards point (a), it should be noted that the climatic regime and in particular the rainfall regime considered in the *FSA* is more variable than that considered in the *SSA*. Figures 5 and 6 show the histograms of the mean values and *L-CS* of the annual extreme rainfalls of duration 12 hours observed in the *FSA*, and the *SSA*, respectively; the higher variability of the *FSA* rainfall statistics is evident. The somewhat higher average rainfall statistics for *FSA* (see Fig. 5) account for an increase in the average value of m_Q.

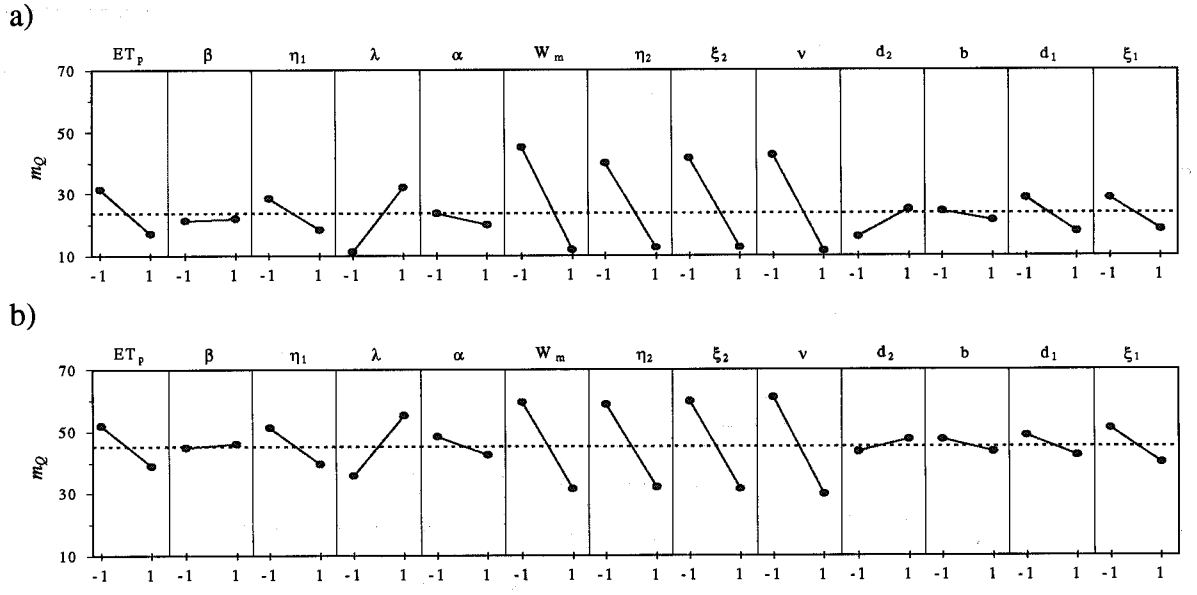

Fig. 4. *Main effect plots for the mean annual flood m_Q: (a) SSA, (b) FSA. The dashed line represents the average value of m_Q observed over all treatment combinations.*

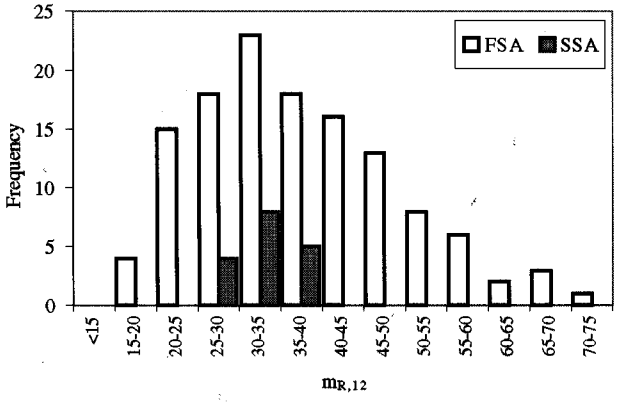

Fig. 5. *Histograms of 12 hr mean annual rainfall maximum values for SSA (total 13 values) and FSA (total 128 values).*

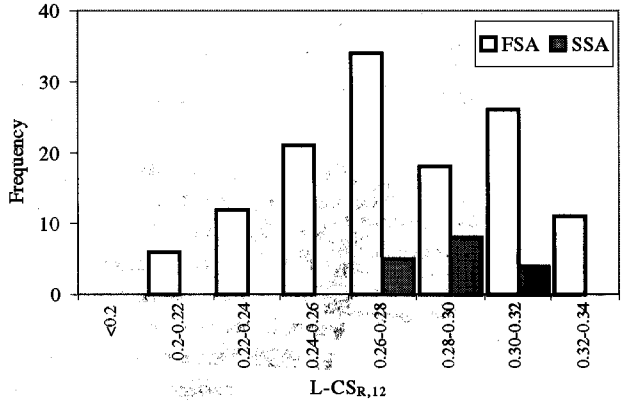

Fig. 6. *Histograms of L-CS of 12 hr annual rainfall maximum values for SSA (total 13 values) and FSA (total 128 values).*

For the explanation of the behaviour highlighted by the points (b) and (c), it is necessary to analyse simultaneously the two-factor interactions shown in Fig. (7). In the main diagonal, the symbols of the different parameters can be read. On the upper line of each matrix, the numbers -1 and $+1$ indicate the lower and the upper level of each parameter, while the values of m_Q are indicated on the right vertical border.

The interpretation of this type of matrix is not straightforward and requires a certain degree of patience. In fact, this matrix is not symmetric. In the upper triangular part it is possible to read, for example, the interaction effect of the parameter η_2 with the parameter d_2: the dashed line represents the *average* effect of d_2 when η_2 is at its upper level and the other parameters can assume *all* their possible combinations, while the solid line represents the *average* effect of d_2 when η_2 is at its lower level and the other parameters can assume *all* their possible combinations.

On the contrary, the *average* effect of η_2 when d_2 is set at its low and high levels is read in the corresponding window in the lower triangular part of the matrix. Thus, this latter window is not 'equal' to the corresponding window in the upper triangular part and the matrix is not symmetric in mathematical/geometrical terms.

Finally, the link between the Fig. 4b and Fig. 7 is identified easily by recalling that the main effects represent an average of the 'system response' over all the considered combinations of all the other parameters, i.e. each window in Fig. 4b can be seen as the average of all the windows in the corresponding column of the two-factor interaction matrix represented in Fig. 7.

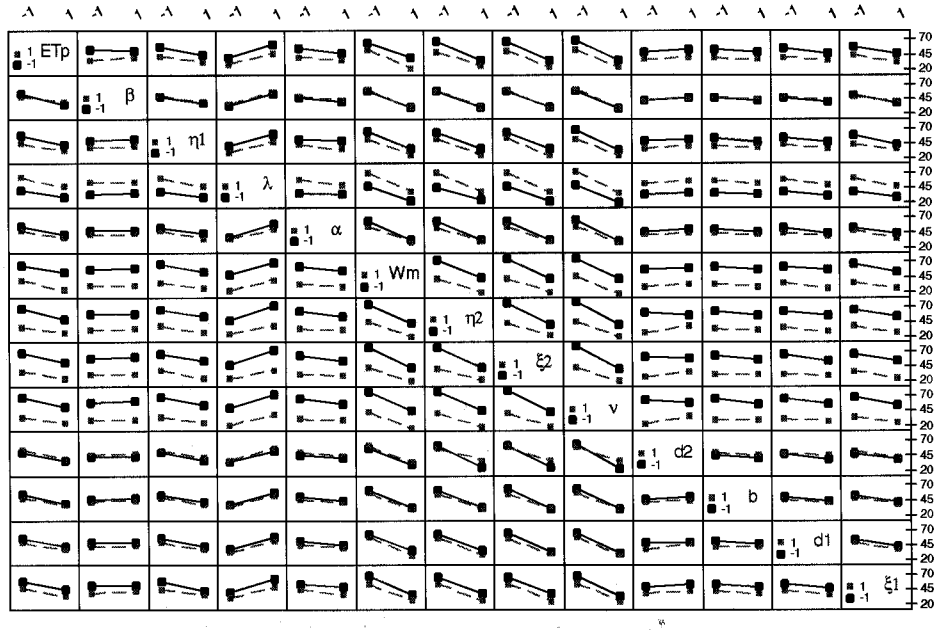

Fig. 7. *Matrix representing the two-factor interaction effects for the mean annual flood m_Q.*

On the basis of the previous considerations, it is now possible to explain the points (b) and (c) above.

As regards point (b), Fig. 7 shows that, for the statistic m_Q, very few two-factor interactions exist. Thus, the slopes of the segments representing the main effects in Fig. 4b are basically equal to those of the corresponding segments of the many cross-interaction windows in Fig. 7 and, at the same time, they are equal to those observed in the *SSA*. This result confirms that all the deductions in Hashemi *et al.* (2000) on the effect that the parameter perturbations have on the position/location and, thus, on the upward/downward shifts of the unstandardised ffcs, were not affected by the reference set used. Furthermore, from a physical point of view, these results imply that each parameter (or rather, each physical aspect represented by the parameter considered) can have a direct effect on the level of the flood regime independently of the values assumed by the other parameters.

Finally, as regards point (c), the effect of each individual parameter is relatively unaffected by the levels of the other parameters (i.e. there are no substantial interactions). Therefore, a main effect calculated from the *FSA*, which is an average over all the other parameter combinations, is similar to that obtained in the *SSA* at the reference set values.

The Pareto chart of the standardised effects for m_Q (Fig. 8) is also worthy of discussion. Even if all the first 30 main effects and two-factor interaction effects are statistically significant at $\alpha = 1\%$, it is evident that the most important are the first eight (main) effects, which relate to the parameters v (controlling the number of cells per storm), ξ_2 (controlling the intensity of the stratiform cells), W_m (controlling soil moisture storage capacity), η_2 (controlling the duration of the stratiform cells), λ (controlling the storm arrival time), ET_p (potential evapotranspiration demand), η_1 (controlling the duration of the convective cells), and ξ_1 (controlling the intensity of the convective cells). Now, independently of the rank of these 8 parameters, it is interesting to observe that the most important factors affecting m_Q are the characteristics of the rainfall regime, potential evapotranspiration demand and the soil moisture storage capacity. Indeed, this information could be useful in the framework of regional flood frequency analysis when a statistical relationship is sought linking the mean annual flood m_Q to some climate and basin characteristics. However, further research is needed on this aspect which has not been considered a main focus of the current research.

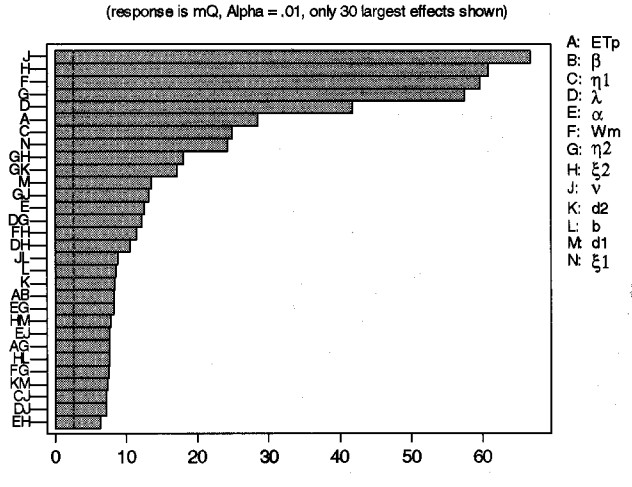

Fig. 8. *Pareto chart of the standardised effects for the mean annual flood m_Q. The dashed line corresponds to a significance level of $p = 0.01$.*

STATISTIC $L\text{-}CS_Q$ (CURVATURE): MAIN EFFECTS AND TWO-FACTOR INTERACTIONS

Figure 9a shows the effects of the different model parameters on the $L\text{-}CS_Q$ statistic observed in the context of the *SSA*. Figure 9b shows the corresponding main effects observed in the *FSA*.

As for the previous case, three different types of consideration can be made:

(a) the level of $L\text{-}CS_Q$ observed in the *FSA* is generally lower than that observed in the *SSA*;
(b) the range of variation of the statistic $L\text{-}CS_Q$ in the *FSA* is clearly smaller than that observed in the *SSA*;
(c) the type of the main effects observed in the *FSA* is not always coherent with the corresponding effect observed in the *SSA*: this applies to the parameters, η_2, ξ_2 and b, and, to some extent, the parameters α, β.

The explanation for these three points can be given through the analysis of the two-factor interaction matrix (Fig. 10) where several substantial interaction effects between the parameters are present.

As regards η_2, ξ_2, Fig. 10 reveals that, in the two columns relevant to these parameters, the two factor interactions dominate and, on average, the main effects are therefore negligible. The marked effect observed in the *SSA* is due to the fact that the type of analysis limits the possibility of parameter combinations and thus it may highlight an effect which is essentially related to the reference set.

Nevertheless, from a physical point of view, one could observe that, when two different cell types are *always* present during a storm, those of stratiform type (i.e. type 2) have a major effect on the lower part of the standardised ffc while those relevant to the convective cells (i.e. type 1) have a major impact on the upper part. Thus, the main effect on the curvature of the ffc is high in the case of the cells of type 1 (see Fig. 9) and low or nil in the case of the cells of type 2. This, however, does not imply that the two parameters η_2, ξ_2 have no effect in general, but that they exert their influence on the ffc curvature through the two-factor interactions.

In the case of the parameter b, the *FSA* produces results which are the reverse of those from the *SSA*. The *FSA*

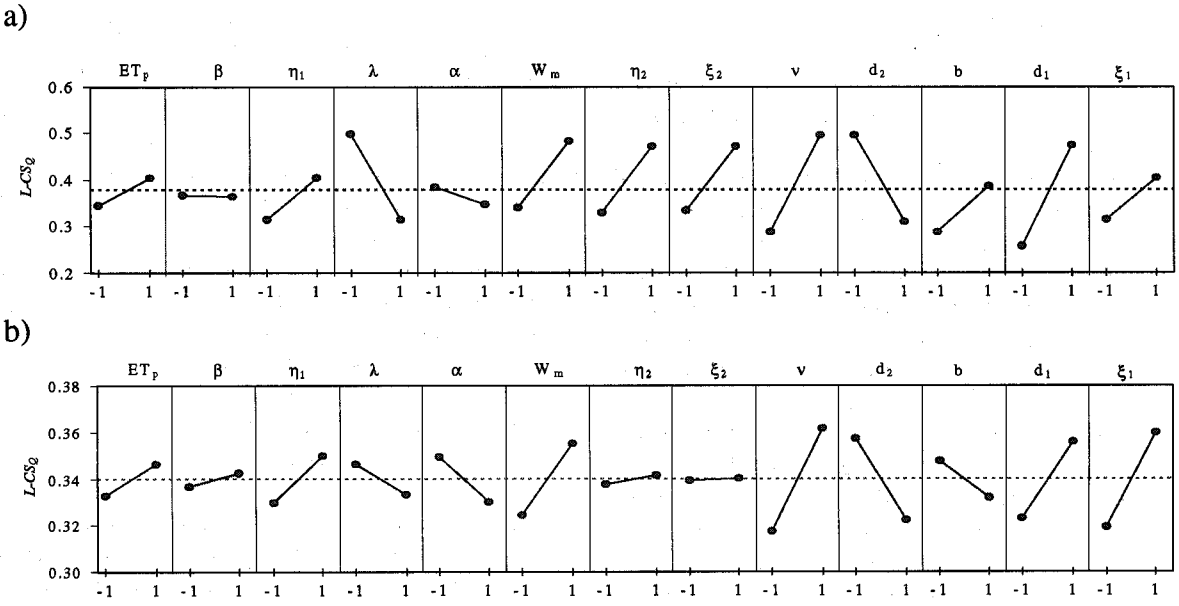

Fig. 9. *Main effect plots for the L-CS$_Q$; (a) SSA, (b) FSA. The dashed line represents the average value of L-CS$_Q$ observed over all treatment combinations.*

identifies a main effect of the parameter b, but also highlights a marked two-factor interaction (Fig. 10) between this parameter and W_m which is perfectly coherent with the structural link mentioned in Hashemi *et al.* (2000). In fact, the analysis of Fig.10 shows that when W_m is high, the variation from the lower to upper bound of the parameter b implies a decrement of the curvature while, when W_m is low, the same variation implies an increment of the curvature.

For the parameter α, the proportion of the convective cells (type 1), the main effect observed in the *FSA* is more marked (and statistically significant) than that observed in the *SSA* and this suggests that the conclusion drawn by Hashemi *et al.* (2000) on the significance of this parameter is restricted to the case where the other parameters are near their reference values, thus highlighting the importance of the *FSA* for revealing more clearly the effects on the ffc characteristics exerted by the individual parameters. The role of the parameter α is confirmed also in terms of two-factor interactions. In fact, Fig. 10 shows, in the α-column, a systematic decreasing trend of the L-CS$_Q$ statistic when the

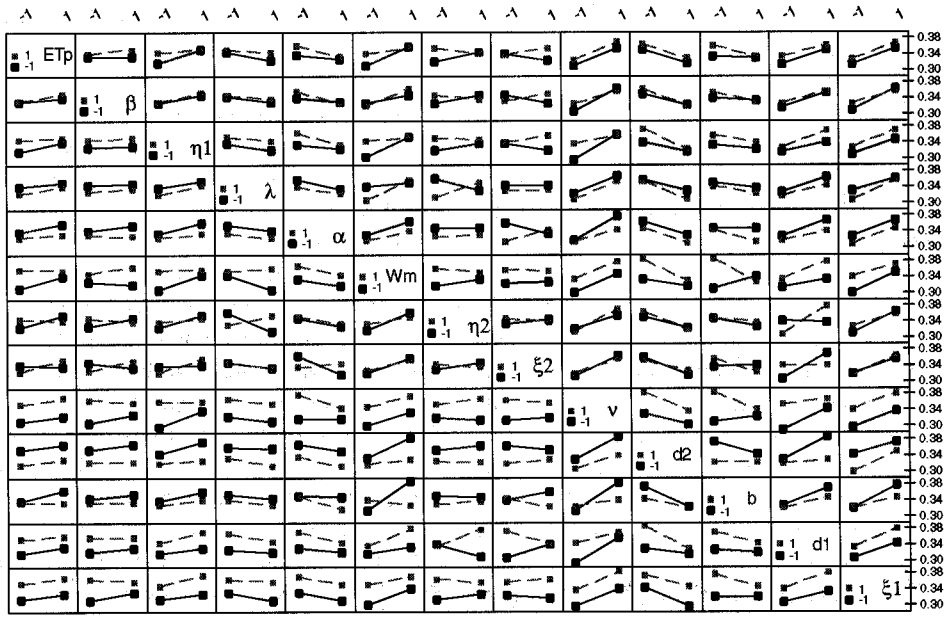

Fig. 10. *Matrix representating the two-factor interaction effects for the L-CS$_Q$.*

parameter α passes from the lower to the upper bound (there is only an exception for the cross-interaction with the parameter ξ_2). This result can be justified from a physical point of view. An increment of α tends to transform all the storm events into events which are similar to *thunderstorms*. In line with the observations made in Hashemi *et al.* (2000), the similarity among all the critical events has the effect of reducing the difference between less extreme and more extreme flood events and, thus, the $L\text{-}CS_Q$ statistic reduces.

Finally, it is confirmed that the parameter β has no main effect on the $L\text{-}CS_Q$ statistic considered, as already highlighted in the *SSA*, even if the (small and statistically not significant) slope of the segment linking the low (−1) and high (+1) average values of $L\text{-}CS_Q$ is reversed with respect to that observed in the *SSA*. Nevertheless, the two-factor interaction matrix shows that this parameter can exert its effect through the interactions with other parameters, as for the case of the parameters η_2, ξ_2 discussed above. However, the analysis of the P statistic, calculated in the framework of the ANOVA (not shown here, as already mentioned) suggests that its effects remain moderate, even at this level.

The above observations globally confirm the results of the *SSA* for the statistic m_Q and $L\text{-}CS_Q$ thus making the conclusions drawn in Hashemi *et al.* (2000) of wider validity and not linked strictly to the selected reference set. Some further information has also been gained on the effect of the parameters α, β, η_2, ξ_2 and b on the $L\text{-}CS_Q$ statistic. Also, the interaction effect of the two parameters W_m and b is now clearly identified.

More generally, the *FSA* has shown that the curvature of the ffc can be affected by two-factor interactions between different pairs of rainfall model parameters, between different pairs of rainfall runoff parameters and between rainfall model parameters, potential evapotranspiration demand and rainfall runoff model parameters (see Figs. 7 and 10). This complex reciprocal influence between climate and basin characteristics suggests further analysis to understand more completely the mechanisms affecting the link between them and the ffc properties.

Further analysis of the results of the experimental design

In Hashemi *et al.* (2000), on the basis of the results of the *SSA*, it has been suggested that the probability distribution of the soil moisture at the storm arrival time has a key role in explaining the link between all the parameters controlling the climate and basin characteristics and the ffc properties. This role is confirmed below by the *FSA*. However, as already mentioned in a previous section, the *FSA* produces a wider variability in the climate regime than that observed in the *SSA* (Figs. 5 and 6). In this particular context, further factors/aspects have to be considered to explain the links between all the parameters controlling the climate and basin soil characteristics and the ffc properties.

CONFIRMATION OF THE ROLE EXERTED BY THE *SAT* SOIL MOISTURE CONTENT PROBABILITY DISTRIBUTION

According to the definition of the main effect of a factor, it is possible to evaluate the average 'system response' for both the lower and upper values of each parameter. Thus, for example, all the synthetic series obtained with $\lambda+$ were combined and several statistics (m_Q, $L\text{-}CV_Q$, $L\text{-}CS_Q$ for annual maximum peaks, and m_{SAT}^{SM}, $L\text{-}CV_{SAT}^{SM}$, $L\text{-}CS_{SAT}^{SM}$ for the soil moisture content at the *SAT*) were then estimated. Finally, for each statistic, the corresponding grand average was calculated.

Figure 11 shows the nine possible plots of the annual maximum discharge statistics, obtained as described above, against soil moisture content statistics at *SAT*. It is evident that all the statistics of the annual maximum peaks are related to the statistics of the soil moisture content at *SAT*. For example, it is shown that m_Q is directly related to m_{SAT}^{SM} and is inversely related to $L\text{-}CV_{SAT}^{SM}$ and $L\text{-}CS_{SAT}^{SM}$. On the other hand, $L\text{-}CS_Q$ is inversely related to m_{SAT}^{SM} and directly related to $L\text{-}CV_{SAT}^{SM}$ and $L\text{-}CS_{SAT}^{SM}$. This implies that higher peak flood values are expected as the soil moisture at *SAT* increases while the curvature of the ffc (related one-to-one to $L\text{-}CS_Q$) is expected to decrease. Overall, the nine plots suggest that, as the mean of the *SAT* soil moisture content probability distribution increases, the L-coefficient of variation gets smaller, the L-skewness become less negative, the discharge value for a given return period increases and an upward shift of the unstandardised ffc is expected but its curvature decreases.

These results confirm what was suggested by the *SSA*. Nevertheless, Fig. 11 represents values that are, as previously mentioned, grand-average values, obtained by combining together the different synthetic series characterised by a selected level of the considered parameter.

FURTHER FACTORS AFFECTING THE LINK BETWEEN ALL THE PARAMETERS CONTROLLING THE CLIMATE AND BASIN CHARACTERISTICS AND THE FFC PROPERTIES

A similar set of nine plots can be obtained when the same statistics are extracted directly from each synthetic series generated in the framework of the designed experiment. The results are shown in Fig. 12. The comparison between this latter figure and Fig. 11 highlights two main aspects: 1) the direct/inverse trends shown in each window are the same in the two figures; 2) the variability of the data observed in Fig. 12 (particularly in some windows) is high and in some case tends to obscure the presence of the trend. This result, which is related mainly to the wider range of the climate regime, suggests that the soil moisture probability distribution indeed exerts an important role in linking the characteristics of the ffcs to the climatic and basin charac-

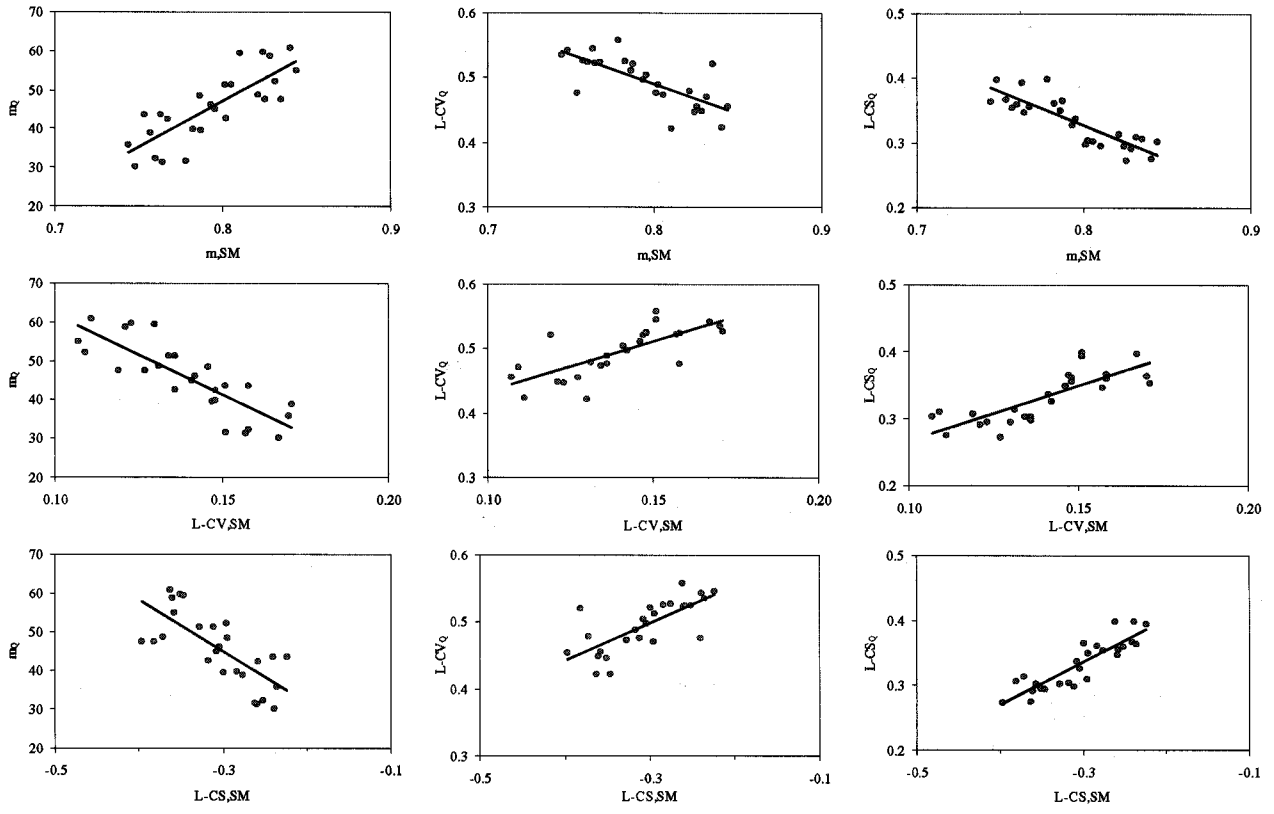

Fig. 11. *Relationships between grand-average statistics of annual maximum flood (Q) and SAT grand average soil moisture content (SM) statistics. (Note: m,SM = m^{SM}_{SAT}, L-CS,SM = L-CS^{SM}_{SAT} and L-CV,SM = L-CVm^{SM}_{SAT}).*

teristics, as shown by the confirmed trends. However, the high variability justifies the search for other mechanisms which, combined with the probability distribution of the soil moisture content at the *SAT*, can explain the observed variability of the data.

An interesting result is shown in Fig. 13, where the plots for the statistic m_Q shown in Fig. 12, are now obtained by considering the statistics estimated only from the synthetic series corresponding to W_m+ and $b-$. In this case the variability is reduced while the trends previously observed are confirmed. Similar results can be obtained for the statistics $L\text{-}CV_Q$ and $L\text{-}CS_Q$. Since fixed values of W_m and b imply that the probability distribution of the soil moisture capacity is fixed, this figure and similar figures for the other three possible combinations of the levels for W_m and b suggest that *the soil moisture content probability distribution at the SAT* still exerts a major influence, but its effect *is conditioned* or affected *by the probability distribution of the soil storage capacity*. On the other hand, this latter probability distribution controls the dynamics of the contributing area, at least within the framework of the rainfall runoff model used. This also means that the dynamics of the soil moisture content affect the flood characteristics through the dynamics of the contributing area.

Due to the wider variability of the climate regime and, in particular, of the rainfall regime produced in the *FSA*, the properties of the rainfall extremes also need to be considered in explaining the variability of the data shown in Fig. 12. Figure 14 shows, for example, a clear statistical relationship between the statistics m_Q, $L\text{-}CV_Q$ and $L\text{-}CS_Q$ and the mean value of the annual maximum rainfall statistics of duration 12 hours. On the other hand, Fig. 15 shows that no statistical relationship exists between the statistics of the rainfall extremes and the statistics of the soil moisture content at *SAT*. Indeed, this latter result was expected, because the soil moisture content at *SAT* is the consequence of the overall climate regime and not of the extreme storm events which occur rarely. These results imply that the statistics of the annual maximum peak flood, and thus the characteristics of the ffcs, are also affected directly by the rainfall extreme characteristics which, however, are not reflected in the probability distribution of the soil moisture content at the *SAT*. Thus the effect of the rainfall extremes can be 'superimposed' on that produced by the soil moisture dynamics, and this can explain the further variability of the data shown in Fig. 12 not explained by the *SAT* soil moisture content and soil moisture capacity probability distributions.

The previous discussion, even if based on qualitative observations of the plots shown in Figs. 12 to 15, is suffi-

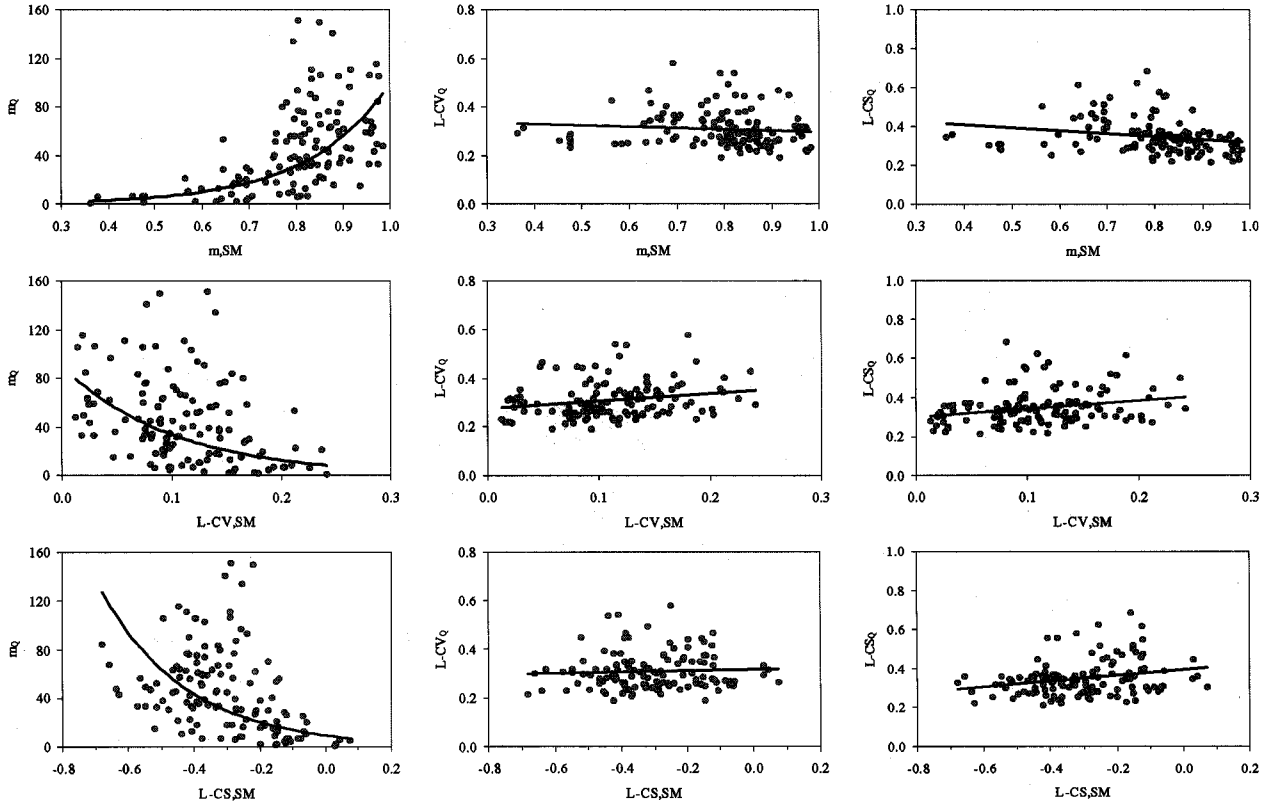

Fig. 12. *Relationships between statistics of annual maximum flood (Q) and SAT average soil moisture content (SM) statistics of individual simulations.*

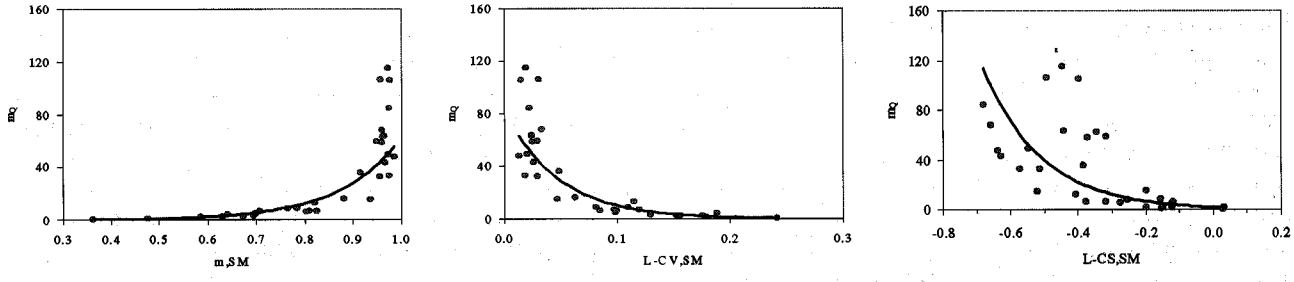

Fig. 13. *Relationships between statistics of annual maximum flood (Q) and SAT average soil moisture (SM) content statistics: case of W_m+ and b−.*

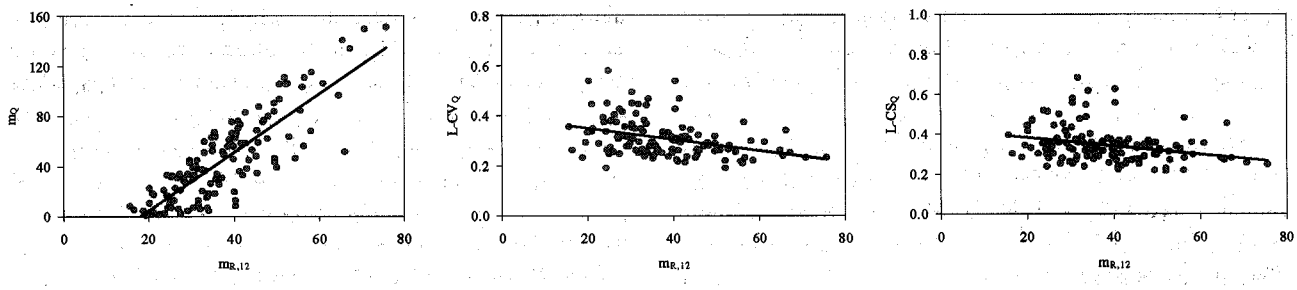

Fig. 14. *Relationships between statistics of 12 hr annual maximum rainfall (R) and annual maximum flood (Q) properties.*

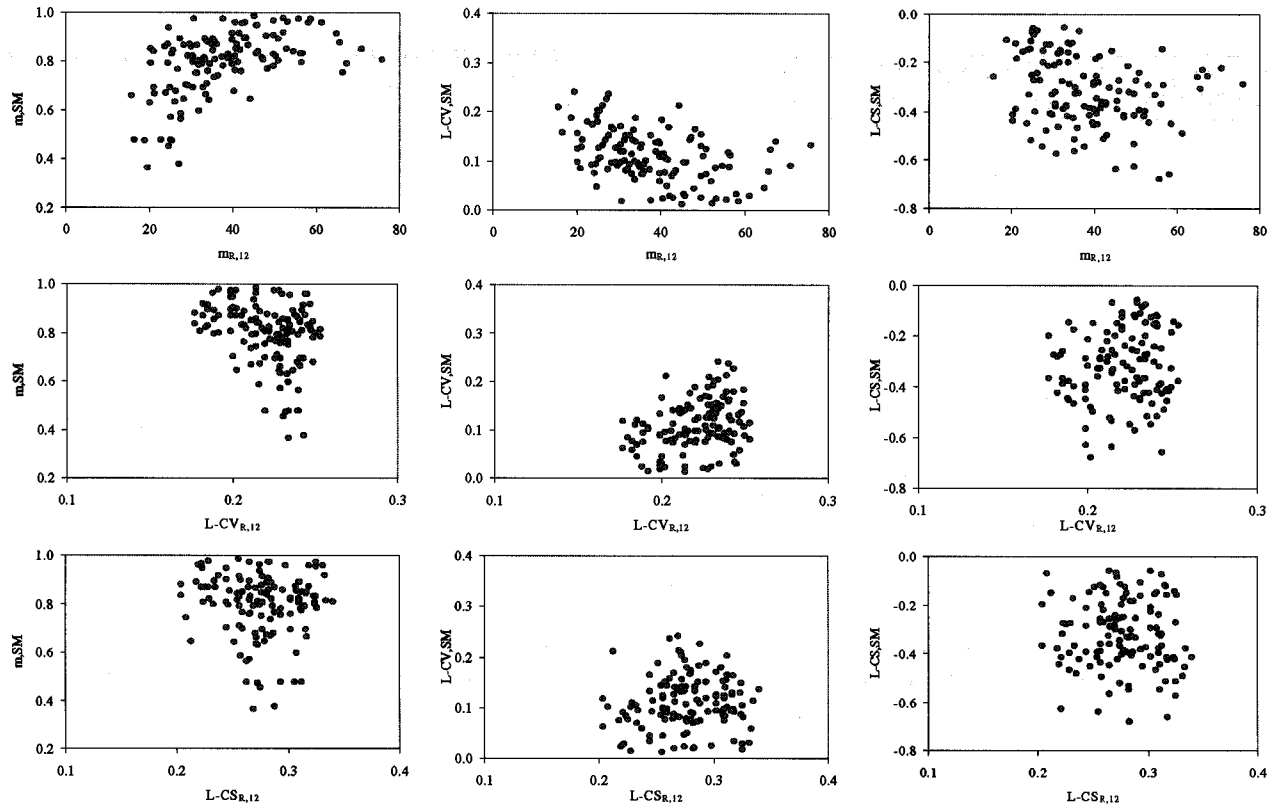

Fig. 15. *Relationships between SAT average soil moisture (SM) content properties and statistics of 12 hr annual maximum rainfall (R).*

cient to demonstrate that the factors affecting the links between all the parameters controlling the climate and basin soil characteristics and the ffc properties cannot be restricted to the soil moisture content probability distribution at the storm arrival time as suggested by the *SSA*. It is, in fact, evident that such a distribution is *conditioned* by the combined effect of the soil moisture capacity (W_m) and its spatial distribution (b) and that the statistics of the annual rainfall extremes are generally correlated with the corresponding statistics of the annual maximum floods.

These results suggest that, for the much wider range of climatic conditions covered by the *FSA*, in comparison with the *SSA*, the relative importance of different factors needs to be further investigated. For example, if a high rainfall regime is combined with a low evaporation regime in the *FSA*, the catchment would be saturated for much of the time and the rainfall factors would dominate. Further research is now being carried out to identify regions of the parameter space where different groups of factors may be dominant or secondary, and, possibly, to identify further factors not highlighted by this study. Moreover, all the climatic conditions represented in the *FSA* will need to be examined, to ensure that they are physically realistic. The parameter perturbations could also be varied throughout the year to explore the effects of changes in seasonality, and different rainfall and evaporation records could also be used in the analysis.

Summary and conclusions

Two major summarising points need to be made concerning the analysis developed in this paper: (1) validation of the effects of the model parameter perturbations on the unstandardised and standardised ffc observed in Hashemi *et al.* (2000); (2) identification of further possible key links between climate/basin soil factors and ffc characteristics.

As regards point (1), the *FSA* globally confirms the results of the *SSA* thus making the conclusions drawn in Hashemi *et al.* (2000) of wider validity and not strictly linked to the reference set selected. The differences observed between the results of the *FSA* and the *SSA*, essentially for the statistic $L\text{-}CS_Q$, have been explained through the analysis of the two-factor interactions. Their presence implies that the effect of one parameter on the standardised ffc can be even reversed depending on the level of the other parameter(s). As a consequence, in real world cases, a particular combination of climatic and soil basin characteristics can produce a ffc, the properties of which can be different from those expected on the basis of the analysis of the main effects alone. This is particularly true for the statistic $L\text{-}CS_Q$ controlling the curvature of the ffc while, for the statistic m_Q, where no two-factor interactions are observed, the analysis of the main effect is sufficient to foresee the effect of each parameter. However, for the

statistic $L\text{-}CS_Q$, the two-factor interactions are present between different pairs of rainfall model parameters, between different pairs of rainfall runoff parameters and between rainfall model parameters, potential evapotranspiration demand and rainfall runoff model parameters. This has suggested that further analysis is needed on the key links between climate/basin factors and ffc characteristics (point 2). The soil moisture content probability distribution at the storm arrival time (*SAT*) has been confirmed as an important conditioning link, as initially suggested by the results of the *SSA*. However, due to the wider range of the climatic behaviour produced within the *FSA*, another two factors/aspects have been identified, namely, the soil moisture capacity probability distribution and extreme rainfall depth characteristics. The soil moisture capacity probability distribution affects the type of soil response in terms of surface runoff/contributing area, thus conditioning the effect of the soil moisture content at *SAT* on the ffc characteristics. As might be expected, the statistics of the rainfall extremes have been shown to be completely uncorrelated with the *SAT* soil moisture content, and so the rainfall extremes affect the ffc directly.

In summary, the full sensitivity analysis (*FSA*) suggests the following conclusions:

(i) the perturbations applied to the rainfall model parameters, potential evapotranspiration demand (time series), or rainfall runoff model parameters (excluding the routing parameters), modify the characteristics of the ffcs;
(ii) the perturbations are always accompanied by modifications to the probability distribution of the soil moisture storage content at *SAT*;
(iii) these modifications have a strong relationship with the ffc characteristics (in particular location and curvature) thus suggesting that the soil moisture content probability distribution at *SAT* can be considered as the physical link between climatic/basin and ffc characteristics;
(iv) however, its effect is *conditioned* by the probability distribution of the soil moisture capacity which, in turn, controls the dynamics of the contributing area generating surface runoff;
(v) a further effect on the statistics of the annual maximum floods, and thus on the ffc characteristics, derives from the characteristics of the annual extreme rainfall depths.

These conclusions have been reached by analysing the time series of several variables generated within the framework of a 2^{k-p}_{IV} fractional factorial experiment where all the model parameters and the potential evapotranspiration demand have been allowed to assume only a low and high value, excluding *a priori* intermediate combinations, which might be very important when the effects of particular hydrological regimes are contrasted. However, the inclusion of intermediate values would have increased greatly the dimensionality of the experiment.

Furthermore, the possible combinations of the two levels assigned to each parameter can produce a rainfall regime (for example very humid) paired unrealistically with soil properties (soil moisture storage capacity distribution and drainage rate) which might be representative of dry regions. It is thus evident that the conclusions presented on the basis of the experimental design are not exhaustive; however, they indicate the presence and the simultaneous influence of three logical blocks of factors representing the soil moisture content at the *SAT*, the soil moisture capacity probability distribution (representing the soil moisture storage/contributing area saturation excess mechanism) and the rainfall extremes. Further research is necessary to gain a better understanding of their relative importance in controlling the flood regimes and to identify possible regions of the parameter space where each of them can be dominant or secondary, and, maybe, to find further aspects/logical blocks of factors not yet highlighted by the current research.

The interpretation of the results produced within the *SSA* and *FSA* frameworks has been limited by the simplified structure of the rainfall runoff model, which, furthermore, excludes *a priori* the Hortonian mechanism of runoff production. To gain a better understanding of the influences of topography, soils, vegetation, geology and geormorphology on the ffc, a more physically-based modelling approach is needed. However, distributed models such as SHETRAN (Ewen *et al.*, 2000) are too computationally demanding for the Monte Carlo simulation approach, and so a more computationally efficient model is needed which can still represent explicitly the above physical factors. *TOPKAPI* (Ciarrapica and Todini, 1998) is a simplified physically-based distributed topographic model which would appear to be suitable for this purpose, particularly since the lumped parameter formulation of the model has been derived directly from the distributed formulation, thus providing the required computational efficiency. Similarly, a computationally efficient hydraulic network simulation model is required which can be used to explore the influence of the hydraulic and topological properties of the channel network, including flood plain storage, on the ffc. An object-oriented numerical model has been developed which is suitable for this purpose (Murray and Kutija, 2000). Moreover, the influence of the spatial variability of rainfall would also need to be included as an additional factor; this can be achieved using the GNSRP space-time model (Cowpertwait, 1995).

By carrying out a further programme of *SSA* and *FSA* experiments using the above modelling tools, a deeper insight into the physical basin factors controlling the ffc will be obtained, enabling the dominant controls in different basins to be identified. This understanding would not only be useful for identifying homogeneous groups of basins for current methods of regional flood frequency analysis, but would open the way to the use of new physically-based methods of flood risk estimation based on the continuous simulation approach.

Acknowledgements

The authors acknowledge the very helpful advice on the experimental design provided by Andrew Metcalfe. The study was carried out under the following research programmes: FRAMEWORK (Flash-flood Risk Assessment under the iMpacts of land use changes and river Engineering WORKs: EC contract n° ENV4-CT97-0529), MURST-COFIN99 'Effetti climatici ed antropici sulla formazione delle piene', and CNR-GNDCI, contract n° 99.01417.PF42, project 'VAPI-RIVERS' (VAlutazione PIene-RIsposta di VERSante). The second author's PhD study was supported by the Ministry of Culture and Higher Education, Iran.

References

Beven, K.J., 1998. Generalised Likelihood Uncertainty Estimation (GLUE), www.es.lancs.ac.uk/rhfg/hfdg.html.

Beven, K.J. and Binley A.M., 1992. The future of distributed models: Model calibration and uncertainty prediction. *Hydrol. Process.*, **6**, 279–298.

Box, G.E.P., Hunter, W.G. and Hunter, J.S., 1978. *Statistics for Experimenters. An Introduction to Design. Data Analysis, and Model Building*. Wiley, New York.

Ciarrapica, L. and Todini E., 1998. *TOPKAPI–Un modello afflussi deflussi applicabile dalla scala di versante alla scala di bacino*. Atti del XXVI Convegno di Idraulica e Costruzioni Idrauliche, Catania, Vol. **II**, 49–60.

Cowpertwait, P.S.P., 1995. A generalized spatial-temporal model of rainfall based on a clustered point process. *Proc. Roy. Soc. Lond., Series A*, **450**, 163–175.

Ewen, J., Parkin, G. and O'Connell, P.E., 2000. SHETRAN: Distributed River Basin Flow and Transport Modelling System, *J. Hydrol. Eng.*, **7**, 250–258.

Freer, J. and Beven, K.J., 1996. Bayesian estimation of uncertainty in runoff prediction and the value of data: An application of the GLUE approach. *Water Resour. Res.*, **32**, 2161–2173.

Hashemi, A.M., Franchini, M. and O'Connell, P.E., 2000. Climatic and basin factors affecting the flood frequency curve: PART 1—A simple sensitivity analysis based on the continuous simulation approach, *Hydrol. Earth System Sci.*, **4**, 463–482.

Hosking, J.R.M. and Wallis, J.R., 1997. *Regional Frequency Analysis*, Cambridge University Press.

Metcalfe, A.V., 1997. *Statistics in Civil Engineering, Arnold Publications of Statistics.*

Montgomery, D.C., 1997. *Design and analysis of experiments*, 4th Edition, Wiley, Chichester, UK.

Montgomery, D.C. and Runger, G.C., 1997. *Applied Statistics and Probability for Engineers*, Wiley, Chichester, UK.

Murray, M.G. and Kutija, V., 2000. *Experience In Object Oriented Design.* Proc. of the IV International Conference (CD-ROM), Hydroinformatics 2000, Iowa, USA.

Spear, R.G., Grieb, T.M. and Shang, N., 1994. Parameter uncertainty and interaction in complex environment models, *Water Resour. Res.*, **30**, 3159–3170.

Zak, S.K., Beven, K.J. and Reynolds, B., 1997. Uncertainty in the estimation of critical loads: a practical methodology, *Soil, Water Air Pollution*, **98**, 297–316.